



Dysregulated ANLN reveals immune cell landscape and promotes carcinogenesis by regulating the PI3K/Akt/mTOR pathway in clear cell renal cell carcinoma

Mingzhu Gao^{a,1}, Zhouting Tuo^{b,1}, Zhiwei Jiang^{b,1}, Zhendong Chen^{a,**},
Jinyou Wang^{b,*}

^a Department of Oncology, Second Affiliated Hospital of Anhui Medical University, Hefei, 230601, China

^b Department of Urology, Second Affiliated Hospital of Anhui Medical University, Hefei, 230601, China

ARTICLE INFO

Keywords:

ANLN
Renal cell carcinoma
Multi-omics
Immune cell
PI3K signalling

ABSTRACT

Background: Abnormal anillin (ANLN) expression has been observed in multiple tumours and is closely associated with patient prognosis and clinical features. In this study, we systematically elucidated the clinical significance and biological roles of ANLN in patients with clear cell renal cell carcinoma (ccRCC).

Methods: We obtained transcriptome and clinical data of patients with ccRCC from public databases. Multi-omics data and clinical samples were combined to analyse the correlation between ANLN expression and the clinical characteristics of patients with renal cancer. Additionally, the immune cell landscape of ANLN expression was evaluated using different immune algorithms in the tumour microenvironment. The tumour-promoting potential of ANLN was confirmed using *in vitro* assays, including CCK8 and Transwell assays.

Results: Bioinformatics analysis showed that ANLN is over-expressed in patients with ccRCC, as validated by clinical samples. Publicly available clinical data suggest that high ANLN expression may indicate poor outcomes in patients with ccRCC. Moreover, biological function analysis revealed a marked enrichment of the cell cycle and PI3K-Akt pathways. The distribution of immune cells, particularly M2 macrophages, differed in patients with ccRCC. Furthermore, ANLN silencing inhibited the proliferation, migration, and invasion of renal cancer cells *in vitro*. After ANLN expression was knocked down in 786-O cells, the protein levels of important PI3K signalling pathway components, including PI3K, Akt, and mTOR, drastically decreased.

Conclusions: These findings suggest that ANLN is dysregulated in renal cancer tissues and promotes tumour progression by activating the PI3K/Akt/mTOR signalling pathway.

1. Introduction

Renal cancer remains a major global public health concern, with trends in its incidence and disease burden varying according to

* Corresponding author.

** Corresponding author.

E-mail addresses: chenzh1001@126.com (Z. Chen), wangjinyou@ahmu.edu.cn (J. Wang).

¹ These authors contributed equally to this work and share first authorship.

economic differences across countries [1]. Clear cell renal cell carcinoma (ccRCC), also known as kidney renal clear cell carcinoma (KIRC), accounts for 80 % of all renal cancer cases and has a poor prognosis [2–4]. Most patients with renal cancer are diagnosed at an advanced stage or with metastasis, as patients typically show no evident clinical symptoms in the early stages [5,6]. Patients with advanced ccRCC respond poorly to chemoradiotherapy, and molecular targeted drugs and immune checkpoint inhibitors have limited therapeutic effects on the overall survival of these patients [7,8]. No superior treatment strategy is currently available for this malignant disease; therefore, it is necessary to investigate personalised treatment strategies for patients with ccRCC by identifying important biomarkers.

Abnormal cell cycle progression is a key characteristic of tumorigenesis, and targeting pericellular phase regulatory proteins may be an important strategy for tumour therapy [9,10]. Anillin (*ANLN*), a gene encoding a 1,125-amino acid protein that is located on chromosome 7p14.2, promotes the cell cycle by binding to GTP-RhoA, actin, and cytokinins, which are crucial regulators of cytokinesis [11]. *ANLN* appears to be closely associated with various biological functions in mammalian cells [12,13], and numerous malignant tumours, including those in lung, pancreatic, colorectal, and breast cancers, exhibit abnormal *ANLN* expression [14–17]. *ANLN* is crucial for tumour cell development [16,18]; it is abnormally expressed in several malignancies and accelerates tumour growth [14,17,19]. Although multiple studies have demonstrated that *ANLN* malfunction promotes the malignant proliferation of tumour cells, the expression pattern and biological functions of *ANLN* in renal cancer remain unknown.

The tumour microenvironment (TME), which is composed of noncancerous cells and substances, can either promote or prevent the development, expansion, and metastasis of tumour cells [20–23]. The TME has attracted considerable clinical and academic interest as a target for cancer therapy [24–26]. Here, we examined the immunological functions and immune cell landscape associated with *ANLN* expression in patients with ccRCC. Furthermore, we evaluated the expression profile and clinical significance of *ANLN* in patients with ccRCC using multi-omics data and clinical samples. Various immunological algorithms have been used to analyse the immune environment involved in *ANLN* expression. The tumour-promoting effects of *ANLN* were validated using an in-vitro assay. The objective of this study was to investigate the biological significance of *ANLN* expression in patients with ccRCC.

2. Materials and methods

2.1. Data collection and analysis

We used publicly available databases that have been described in detail in previous studies [27]. First, we downloaded a standardised pan-cancer dataset from the UCSC (<https://xenabrowser.net/>) and GENT2 (<http://gent2.appex.kr/gent2/>) databases [28,29]. Additionally, 33 tumour cell line expression data were downloaded from the Cancer Cell Line Encyclopedia (<https://sites.broadinstitute.org/ccle>) [30]. Subsequently, RNA sequencing and clinical data were obtained from the UCSC database for 527 patients with KIRC. Finally, UALCAN (<http://ualcan.path.uab.edu>) and DriverDBv3 (<http://ngs.ym.edu.tw/driverdb>) databases were used for clinical feature and prognostic analyses [31,32].

2.2. Correlation analysis with heterogeneity and mutation profiles analysis

We examined the relationship between *ANLN* expression and eight types of heterogeneity: homologous recombination deficiency (HRD), loss of heterozygosity (LOH), neoantigen (NEO), tumour ploidy, tumour purity, mutant-allele tumour heterogeneity (MATH), tumour mutation burden (TMB), and microsatellite instability (MSI) [33]. The “maftools” package and MuTect2 software were used to further analyse these data, which were retrieved from the Genomic Data Commons website (<https://portal.gdc.cancer.gov/>) [34,35].

2.3. Univariate and multivariate cox regression analysis

The prognostic significance of *ANLN* expression in patients with ccRCC was analysed using the “survival” and “survminer” packages. We conducted univariate and multivariate Cox regression analyses to ascertain the clinical significance of *ANLN* expression in patients with ccRCC.

2.4. Gene co-expression analysis and biological function analysis

Genes co-expressed with *ANLN* were identified in patients with ccRCC using the “limma” package (P -value < 0.05 and $|\log_2(\text{Fold Change})| > 1$), and biological functions were examined using the R package “clusterProfiler” [36]. These methods have been described in detail in previous studies [37,38].

2.5. Immune cell infiltration analysis

We obtained immune cell data from tumour samples and calculated the correlation between *ANLN* and immune invasion score in tumour samples using the “psych” package. The correlation between *ANLN* expression and the immune landscape was evaluated using the “limma” and “tidyverse” packages in conjunction with the CIBERSORTS tool [39,40].

2.6. Immunotherapy sensitivity analysis

The immunotherapy response in patients with ccRCC was predicted using data from The Cancer Immunome Atlas database [41]. Moreover, drug sensitivity analysis was conducted using the “pRRophetic” package and “ggplot2” tools [42].

2.7. Collecting clinical samples

The Ethics Committee of the Second Affiliated Hospital of Anhui Medical University granted its approval for this study (SL-YX2022-065 [F1]), which was carried out in accordance with the Declaration of Helsinki’s principles. From January 2020 to June 2022, clinical samples and data from 100 renal cancer and adjacent tissues were collected retrospectively at our medical centre after obtaining written informed consent from all patients.

2.8. Immunohistochemistry (IHC) analysis

The tissue samples were sectioned, and experiments were performed using an IHC kit (cat. SP-9001; ZSGB-BIO, China). Following sample preparation, antigen retrieval, and blocking, ANLN (1:100; Affinity Bio., USA) and CD163 (1:100; Abcam, UK) protein expressions were examined using primary and specific secondary antibodies (Biyotime, China). Finally, the staining quantity and intensity were comprehensively analysed as low/negative (≤ 4 points) or high (> 4 points).

2.9. Constructs and cell transfection

We purchased 786-O and ACHN cell lines from Procell Life Science & Technology Ltd. (Wuhan, China), and targeted ANLN short hairpin RNA (shRNA) and a negative control from GenePharm (Shanghai, China). The sequence of ANLN-shRNAs was listed: shANLN-1: 5'-TCCTGGGAAGAT

GATGTAATTTCAAGAGAATTTACATCATCTTCCCAGGATT-3'; shANLN-2: 5'-ATGGCGA
TGCCTCTTTGAATATTCAAGAGATATTCAAAGAGGCATCGCCATTT-3'; shNC: 5'-TTCTCC
GAACGTGTCACGTTTCAAGAGAACGTGACACGTTTCGTCGGAGAATT-3'.

2.10. Quantitative real-time reverse-transcription polymerase chain reaction (qRT-PCR) assay

Total RNA was extracted using TRIzol reagent and reverse transcribed into complementary DNA using a reverse transcription kit (Novabio, China). Following qRT-PCR, the results were analysed using the $2^{-\Delta\Delta Ct}$ method. The primer sequences are listed in Table 1.

2.11. Cell proliferation assay

Cell proliferation was assessed using a CCK8 kit, and 3,000 cells were seeded into each well of a 96-well plate. After 0, 24, 48, 72, and 96 h, the optical density was determined at 450 nm (Thermo Fisher Scientific, USA).

2.12. Transwell assay

Transwell chambers (Corning Inc., USA) were used for Transwell assays. A total of 2×10^5 cells were inoculated into the upper chamber for approximately 24 h, and medium containing 10 % foetal bovine serum was added to the lower chamber. For the invasive assay, 50 μ L Matrigel (Corning Inc., USA) was added to the upper chamber, with all other steps being the same. Finally, the cells were fixed, stained, and photographed (Leica Corporation).

2.13. Western blot assay

Protein sample preparation and western blotting were performed as previously described [43]. Protein samples were separated using sodium dodecyl sulphate-polyacrylamide gel electrophoresis and transferred to polyvinylidene fluoride (PVDF) membranes. The PVDF membrane was blocked with milk and subsequently incubated with primary antibodies against glyceraldehyde 3-phosphate dehydrogenase (1:1000; Affinity, USA), PCNA (1:1000; CST. Inc., USA), cyclin B1 (1:1000; CST. Inc., USA), Akt antibody (1:1000; CST. Inc., USA), PI3K (1:1000; CST. Inc., USA), and anti-mTOR (1:1000; CST. Inc., USA). The membranes were then incubated with

Table 1
Primer sequences used for qRT-PCR amplification.

Gene	Forward primer (5'→3')	Reverse primer (5'→3')
ANLN	CAGACAGTTCATCCAAGGGAG	CITGACAACGCTCTCCAAGCG
GAPDH	GTCTCCTCTGACTTCAACAGCG	ACCACCTGTTGCTGTAGCCAA

qRT-PCR, quantitative real-time polymerase chain reaction.

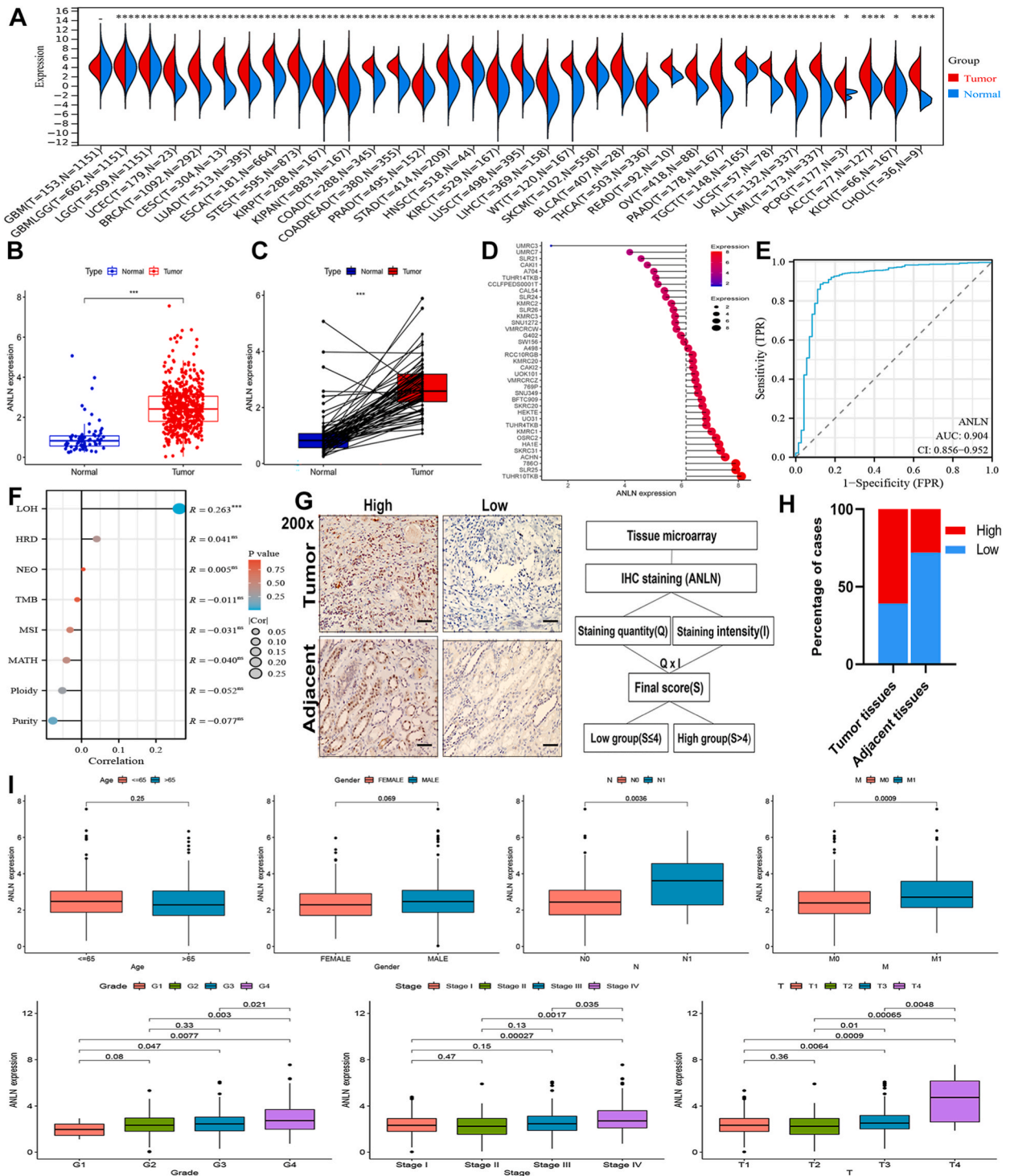


Fig. 1. ANLN is overexpressed in renal cancer. (A) Pan-cancer analysis of ANLN expression in human cancers. Unpaired (B) and paired (C) expression data analyses indicated that ANLN expression was markedly higher in patients with ccRCC. (D) ROC analysis of ANLN expression in the diagnosis of patients with ccRCC. (E) ANLN expression in renal cancer cell line and normal cell line based on the CCLE database. (F) Correlation between tumour heterogeneity and ANLN expression in patients with ccRCC. (G) Representative pictures of IHC staining of ANLN in tumour and matched adjacent normal tissues (magnification: 200 ×). (H) Quantitative and percentage analysis of ANLN staining in tumour and adjacent normal tissues. (I) Correlation between ANLN expression and several clinical features in patients with ccRCC. ANLN = anillin; ccRCC = clear cell renal cell carcinoma; ROC = receiver operating characteristic curve; CCLE = Cancer Cell Line Encyclopedia; IHC = immunohistochemistry.

horseradish peroxidase-conjugated goat anti-rabbit IgG (1:10000; Affinity Bio., USA) and goat anti-mouse IgG (1:10000; Affinity Bio., USA) secondary antibodies. The results were analysed using an ECL kit (Thermo Fisher Scientific).

2.14. Statistical analysis

R (version 4.2.1) was used for data analysis. All continuous data were tested for normality and compared between multiple groups using one-way analysis of variance. Data between the two groups were compared using either the *t*-test or chi-square test. Statistical significance was set at $P < 0.05$.

3. Results

3.1. Expression analysis and clinical significance of ANLN expression in renal cancer

We investigated the expression patterns of *ANLN* in 34 tumour and normal samples and observed that *ANLN* was up-regulated in almost all tumour tissues, except glioblastoma multiforme, based on a pan-cancer dataset from the TCGA database (Fig. 1A). According to the pan-cancer dataset from the GENT2 database, *ANLN* was found to be up-regulated in 24 human tumour tissues (Fig. S1A). Using unpaired and paired analyses, we examined *ANLN* expression in ccRCC tumour and normal samples (Fig. 1B and C), and found that *ANLN* expression increased in almost all tumour cell lines, with the highest expression observed in brain lower-grade glioma cell lines (Fig. S1B). Fig. 1D shows the *ANLN* expression levels in 35 renal carcinoma cell lines and two normal cell lines. Additionally, receiver operating characteristic curve (ROC) analysis revealed decreased *ANLN* expression in patients with ccRCC (AUC: 0.904) (Fig. 1E). *ANLN* expression was positively correlated with LOH ($P < 0.01$), HRD, and NEO in terms of tumour heterogeneity, but negatively correlated with TMB, MSI, MATH, ploidy, and purity (Fig. 1F). To validate these results, we collected 100 renal cancer tissue samples and performed IHC analysis. The results suggested that *ANLN* expression was enhanced in tumour tissues (Fig. 1G and H). The clinical information is shown in Table 2 and Table S1. N stage, M stage, grade, clinical stage, and T stage were statistically significant (Fig. 1I). Similarly, *ANLN* expression varied according to the sample type, individual cancer stage, patient race, patient sex, patient age, tumour grade, nodal metastasis status, and KIRC subtype in the UALCAN database (Fig. S2).

3.2. Independent prognostic value of ANLN expression in patients with ccRCC

Based on publicly available clinical data, increased *ANLN* expression may indicate poor prognosis in patients with ccRCC. Using the DriverDBv3 database, we found that higher *ANLN* expression was associated with worse overall survival, progression-free interval, and disease-specific survival, but not with disease-free interval, in patients with ccRCC (Fig. 2A). Univariate Cox regression analysis

Table 2
Clinical characteristics and follow-up data for our patients with renal cancer.

Variable	Value	High	Low/Negative	P-value	
Total (%)	100	61 (61.00)	39 (39.00)		
Age, years	≥60	33 (33.00)	18 (54.54)	15 (45.46)	0.353
	<60	67 (67.00)	43 (64.18)	24 (35.82)	
Gender	Male	64 (64.00)	40 (62.50)	24 (37.50)	0.682
	Female	36 (36.00)	21 (58.33)	15 (41.67)	
Location	Left	47 (47.00)	28 (59.57)	19 (40.43)	0.596
	Right	52 (52.00)	32 (61.54)	20 (38.46)	
	Bilateral	1 (1.00)	1 (100.00)	0	
Tumor subtypes	ccRCC	85 (85.00)	54 (63.53)	31 (36.47)	0.465
	pRCC	9 (9.00)	4 (44.44)	5 (55.55)	
	cRCC	6 (6.00)	3 (50.00)	3 (50.00)	
Pathologic tumor stage	Ta-T1	48 (48.00)	32 (66.67)	16 (33.33)	0.002
	T2-T3	30 (30.00)	11 (36.67)	19 (63.33)	
	T4	22 (22.00)	18 (81.82)	4 (18.18)	
Lymph node status	N0	9 (9.00)	6 (66.67)	3 (33.33)	0.588
	≥N1	5 (5.00)	4 (80.00)	1 (20.00)	
	Nx	86 (86.00)	51 (59.30)	35 (40.70)	
Metastasis status	M0	0 (0.00)	0	0	1.00
	≥M1	1 (1.00)	1 (100.00)	0	
	Mx	99 (99.00)	60 (60.61)	39 (39.39)	
Tumor size, cm	<4	40 (40.00)	23 (57.50)	17 (42.50)	0.147
	4–7	23 (23.00)	18 (78.26)	5 (21.74)	
	>7	37 (37.00)	20 (54.05)	17 (45.95)	
Recurrence	Yes	9 (9.00)	6 (9.84)	3 (7.69)	0.715
	No	91 (91.00)	55 (90.16)	36 (92.31)	
Current status	Death	3 (3.00)	2 (3.28)	1 (2.56)	0.838
	Alive	97 (97.00)	59 (96.72)	38 (97.44)	

RCC, renal cell carcinoma; ccRCC, clear cell RCC; pRCC, papillary RCC; cRCC, chromophobe RCC.

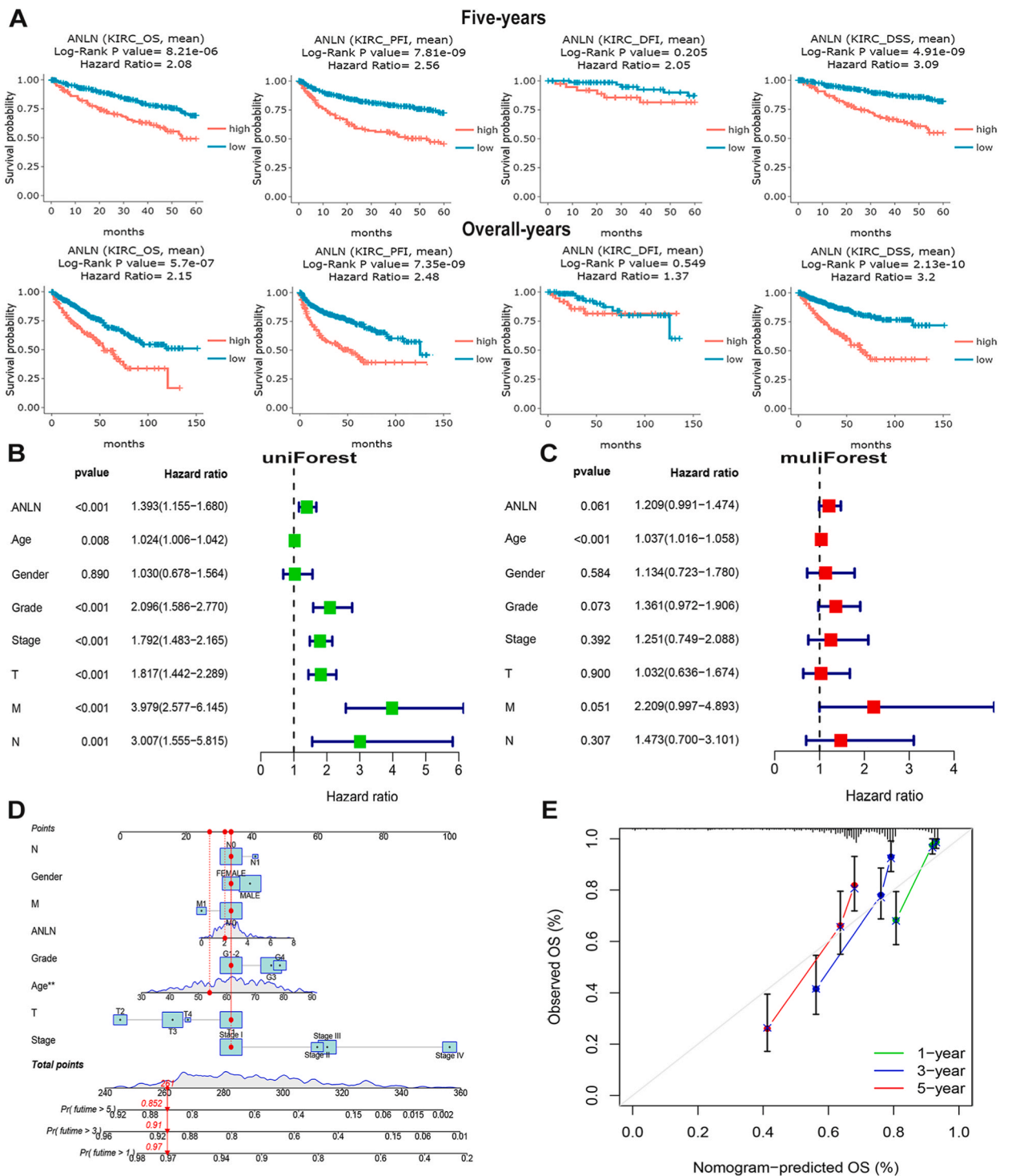


Fig. 2. Analysis of the prognostic value of ANLN expression in patients with ccRCC. (A) Five-year and overall survival analysis of ANLN expression in patients with ccRCC. Univariate (B) and multivariate (C) Cox regression analysis showed that ANLN was an independent risk factor correlated with survival in patients with ccRCC. (D) A prognostic nomogram with ANLN and clinical variables was constructed. (E) The 1-, 3- and 5-year calibration plots show the performance of the nomogram. ANLN = anillin; ccRCC = clear cell renal cell carcinoma.

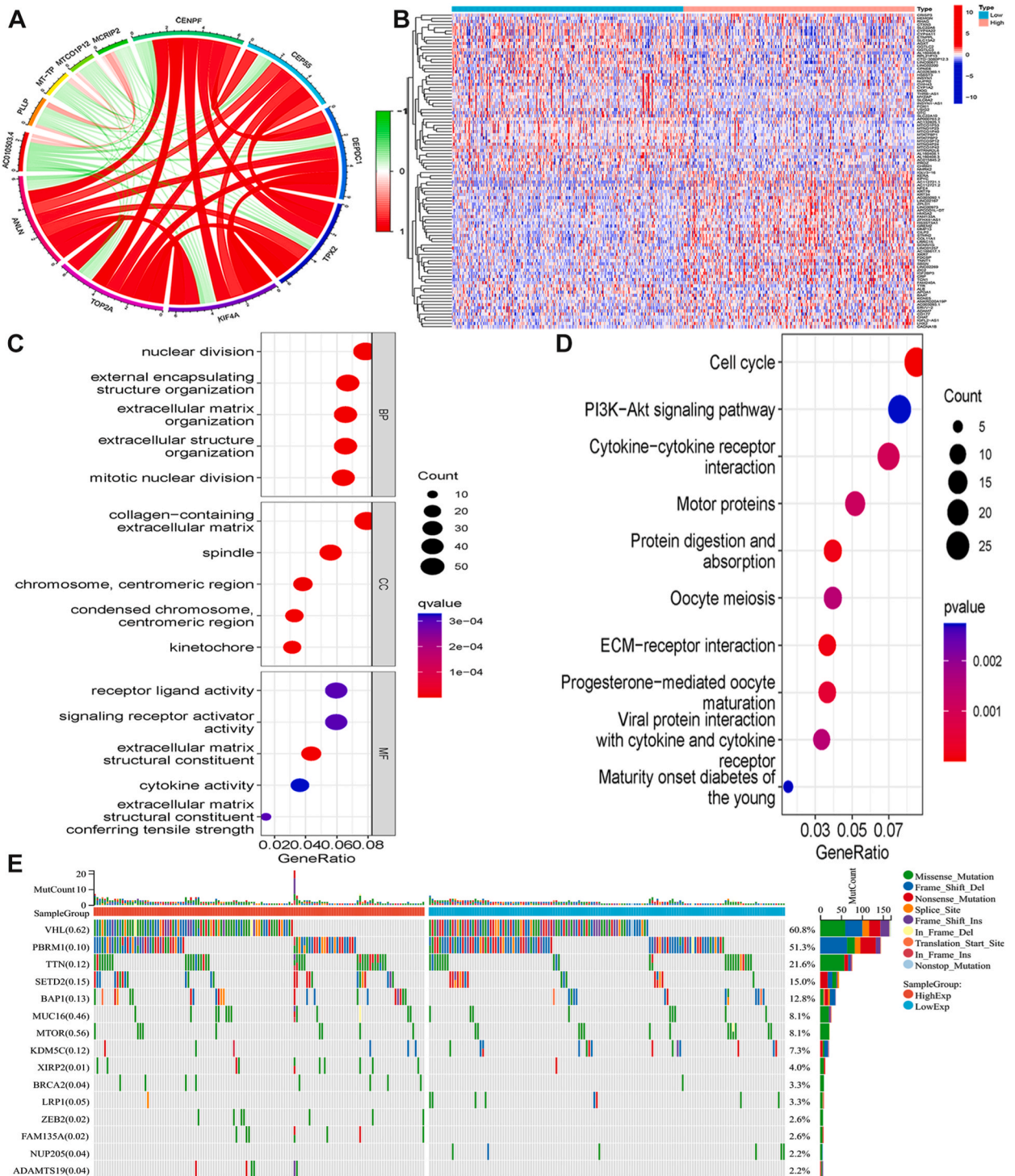


Fig. 3. Biological function and mutation profiles of ANLN in ccRCC. (A) Co-expressed genes significantly associated with ANLN were shown as correlation circle plots. Red, positive correlation; green, negative correlation. (B) Heatmap showing the top 50 up-regulated DEGs and top 50 down-regulated DEGs; red, up-regulated genes; blue, down-regulated genes. (C) GO analysis results of ANLN expression in ccRCC. (D) KEGG analysis results of ANLN expression in ccRCC. (E) The mutation profiles of 15 genes in patients with ccRCC with low and high ANLN expressions. ANLN = anillin; ccRCC = clear cell renal cell carcinoma; DEGs = differentially expressed genes; GO = gene ontology; KEGG = Kyoto Encyclopedia of Genes and Genomes. (For interpretation of the references to color in this figure legend, the reader is referred to the Web version of this article.)

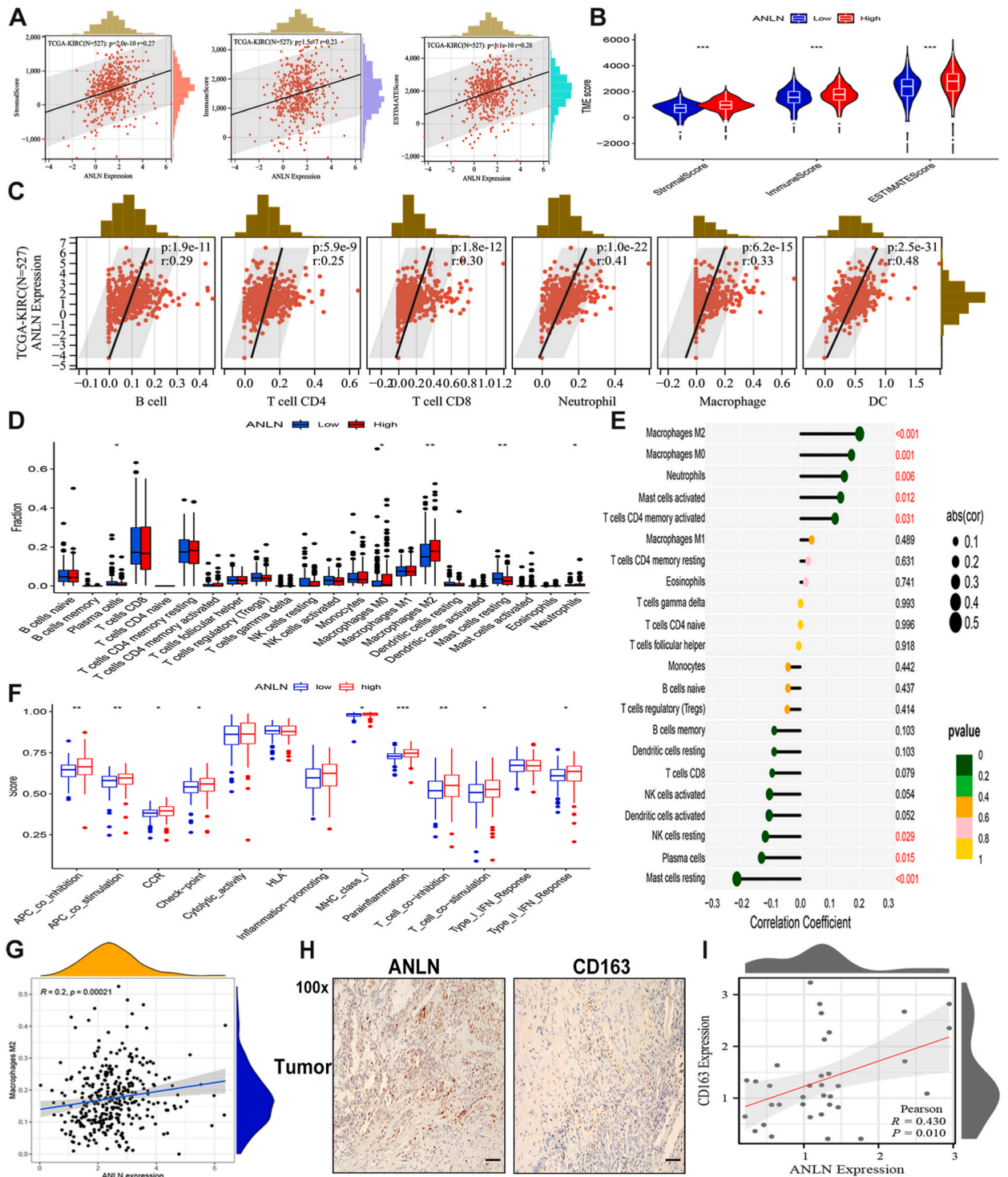


Fig. 4. Dysregulated ANLN reveals the immune cell landscape for patients with ccRCC. (A) Correlation between ANLN expression and three types of microenvironment scores in patients with ccRCC. (B) Three types of microenvironment scores in patients with ccRCC with low and high ANLN expressions. (C) Correlation between six immune cells and ANLN expression in patients with ccRCC based on the TIMER method. (D) Proportion of 22 immune cells infiltrating in low and high ANLN expression groups. (E) Relationships between the expression of ANLN and 22 types of immune-infiltrating cells. (F) Correlations between ANLN expression and various immune functions. (G) Correlation between ANLN expression and macrophage M2 infiltration in patients with ccRCC. (H) Representative images of IHC staining of ANLN and CD163 expression in 35 ccRCC tissues (magnification: 100 ×); (I) Correlation between ANLN and CD163 expression in patients with ccRCC. ANLN = anillin; ccRCC = clear cell renal cell carcinoma; IHC = immunohistochemistry.

showed that *ANLN* expression and several other characteristics had a negative effect on patient prognosis, but only age affected patient survival in multivariate analysis (Fig. 2B and C). Subsequently, we constructed a prognostic nomogram combining the clinical features and *ANLN* expression based on the above results (Fig. 2D). The 1-, 3-, and 5-year survival calibration curves of these patients demonstrated the performance of our model (Fig. 2E).

3.3. Biological function and mutation profiles of *ANLN* expression in patients with ccRCC

We found genes that were either positively or negatively co-expressed with *ANLN* in patients with ccRCC to explore the possible

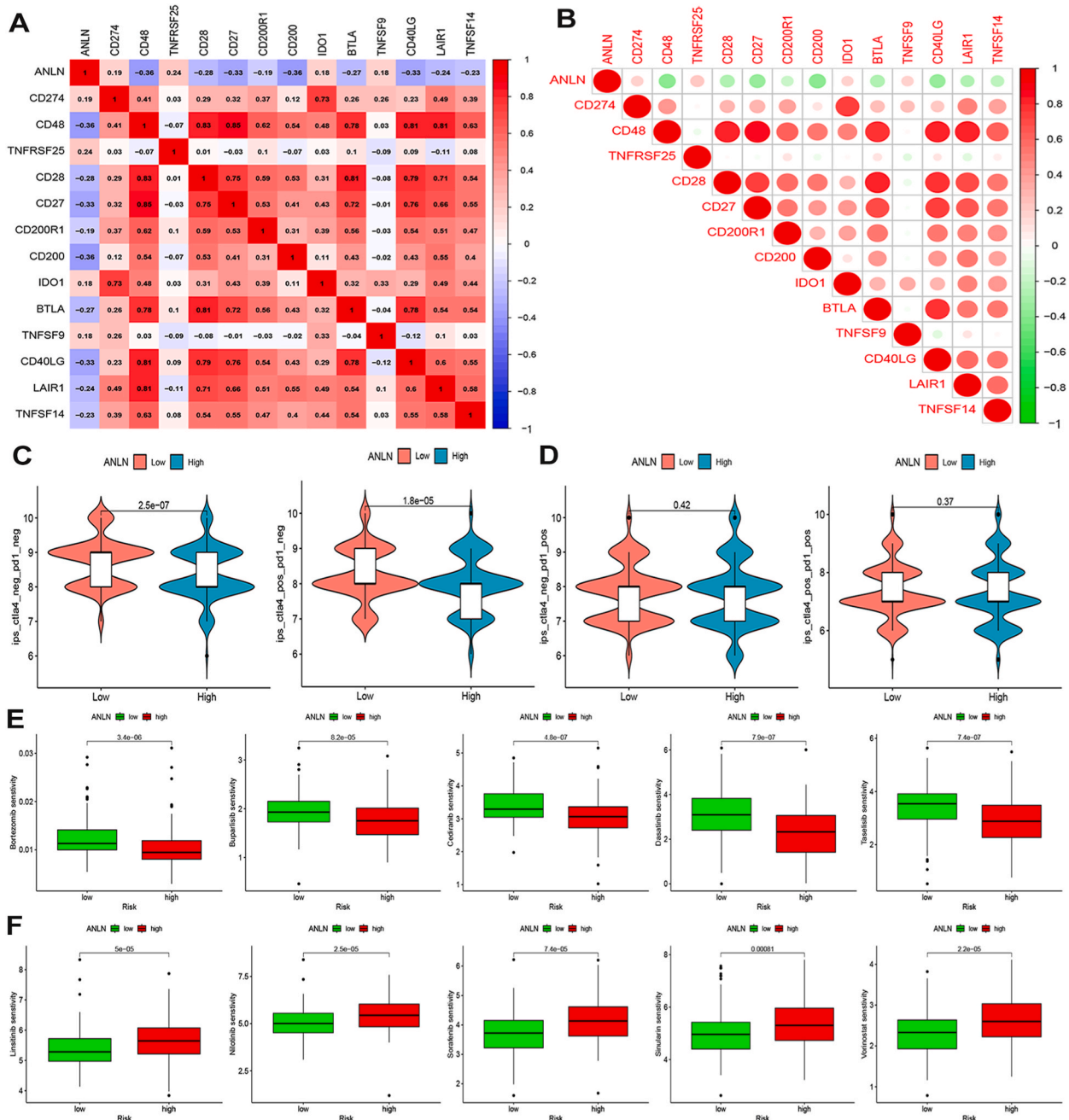


Fig. 5. Role of *ANLN* in immunotherapy response. (A) and (B) correlation between ICIs and *ANLN*. (C) Correlation between *ANLN* expression and immune response score of PDI¹⁻ patients. (D) Correlation between *ANLN* expression and immune response score in ccRCC patients. (E) Sensitivity analysis of bortezomib, buparlisib, cediranib, dasatinib, and taselisib in patients with ccRCC. (F) Sensitivity analysis of linsitinib, nilotinib, sorafenib, sinularin, and vorinostat in patients with ccRCC. *ANLN* = anillin; ccRCC = clear cell renal cell carcinoma.

roles of this protein. (Table S2). In patients with ccRCC, the top ten co-expressed genes were either positively or negatively correlated with *ANLN* expression (Fig. 3A). The top 50 up-regulated and 50 down-regulated genes were screened using a heat map (Fig. 3B). In Gene Ontology analysis revealed that nuclear division, external encapsulating structure organisation, extracellular matrix organisation, spindle formation, receptor ligand activity, signalling receptor activator activity, and extracellular matrix structural constituents were significantly enriched in these patients (Fig. 3C). In the Kyoto Encyclopedia of Gene and Genome analysis, the cell cycle, PI3K-Akt signalling pathway, cytokine-cytokine receptor interaction, and motor proteins were significantly enriched in these patients (Fig. 3D). In patients with ccRCC, substantial genetic mutations were observed between *ANLN* high- and low-groups, including *VHL*, *PBRM1*, *TTN*, *SETD2*, *BAP1*, *MUC16*, *MTOR*, *KDM5C*, *XIRP2*, *BRCA2*, *LRP1*, *ZEB2*, *FAM135A*, *NUP205*, and *ADAMTS19* (Fig. 3E).

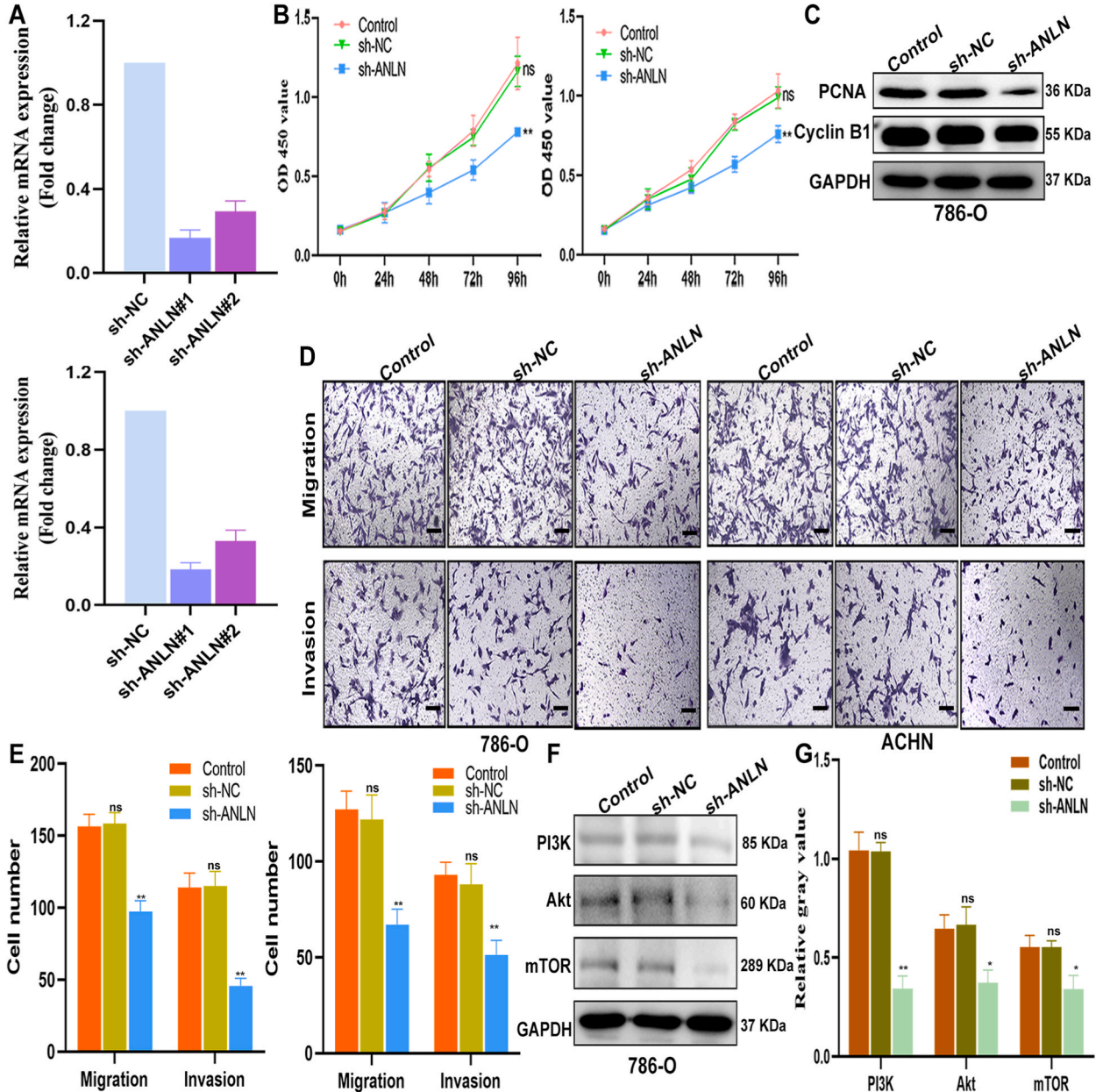


Fig. 6. Effects of *ANLN* silencing on the carcinogenesis of renal cancer cell lines. (A) *ANLN* silencing by targeted shRNA was confirmed using qRT-PCR. (B) Proliferation of renal cancer cells detected using CCK8 assays. (C) Western blotting analysis of PCNA and cyclin B1 expression in 786-O cells. (D) and (E) Representative images of migration and invasion assays (100 ×) and quantification analysis in renal cancer cells. (F) and (G) Western blotting and quantification analyses detected PI3K, Akt, and mTOR in 786-O cells. *ANLN* = anillin; qRT-PCR = quantitative real-time reverse-transcription polymerase chain reaction; shRNA = short hairpin RNA.

3.4. Immune landscape analysis of *ANLN* expression in patients with ccRCC

The crosstalk between TME and cancer cells has attracted considerable research interest [44,45]. We found that *ANLN* expression in patients with ccRCC was positively correlated with stromal, immune, and ESTIMATE scores (Fig. 4A). Moreover, significant differences were observed between the three scores in groups with high and low *ANLN* expression (Fig. 4B). Subsequently, we investigated the association between *ANLN* expression and the infiltration of six types of immune cells using the TIMER method (Fig. 4C). The percentages of 22 immune cell types in patients with ccRCC were determined using the CIBERSORT algorithm. Difference analysis showed the distribution of immune-infiltrating cells based on *ANLN* expression, such as plasma cells, M0 macrophages, M2 macrophages, resting mast cells, and neutrophils (Fig. 4D). *ANLN* expression was significantly positively correlated with M2 macrophages, M0 macrophages, neutrophils, activated mast cells, and activated CD4 memory T cells, but negatively correlated with resting natural killer cells, plasma cells, and resting mast cells (Fig. 4E). The immune cell status was determined using several common algorithms (Fig. S3A–B) according to *ANLN* expression in patients with ccRCC. Furthermore, we found that *ANLN* expression was strongly associated with a range of immune functions in patients with ccRCC (Fig. 4F). The association between *ANLN* expression and macrophage M2 infiltration has been focused on these immune cells (Fig. 4G). From our sample cohort, we selected 35 ccRCC tissue samples for correlation analysis. The results showed that *ANLN* and CD163 expression (a macrophage M2 marker) were positively correlated in patients with ccRCC (Fig. 4H and I).

3.5. Correlation between immunotherapy drug sensitivity and *ANLN* expression in patients with ccRCC

We performed correlation analysis to assess the role of immune checkpoints in patients with ccRCC. According to our findings, *ANLN* was negatively correlated with some immune checkpoint inhibitors (ICIs), such as CD48, CD28, CD27, CD200R1, CD200, BTLA, CD40LG, LAIR1, and TNFSF14, while exhibiting a positive correlation with other ICIs, such as CD247, TNFRSF25, IDO1, and TNFSF9 (Fig. 5A and B). Subsequently, we predicted the effect of *ANLN* expression on immunotherapy. Abnormal *ANLN* expression may affect the efficacy of immunotherapy in PD1⁻ patients; however, no difference was observed in PD1⁺ patients (Fig. 5C and D). For anticancer drugs, patients with ccRCC with low *ANLN* expression showed high sensitivity to bortezomib, buparlisib, cediranib, dasatinib, and tasiselisib (Fig. 5E), whereas patients with ccRCC with high *ANLN* expression showed high sensitivity to drugs such as linsitinib, nilotinib, sorafenib, sinularin, and vorinostat (Fig. 5F).

3.6. Validation of the biological function of *ANLN* in a renal cancer cell line

The tumour-promoting effects of *ANLN* were validated in a renal cancer cell line. Two shRNA knockout cell models were constructed and used in subsequent experiments. *ANLN* expression was noticeably suppressed in 786-O and ACHN cells (Fig. 6A), and silencing of *ANLN* weakened cancer cell proliferation in both cell lines (Fig. 6B). Furthermore, *ANLN* silencing reduced the expression of PCNA and cyclin B1 in 786-O cells (Fig. 6C) and attenuated the migration and invasion abilities of these cells (Fig. 6D and E). After *ANLN* expression was knocked down in 786-O cells, the protein levels of important PI3K signalling pathway participants, such as PI3K, Akt, and mTOR, were drastically decreased (Fig. 6F and G).

4. Discussion

Patients with advanced ccRCC do not respond to targeted therapy or immunotherapy owing to the lack of specific targets [46]. Previous studies have shown that *ANLN* expression is substantially correlated with the prognosis of patients with multiple solid tumours [14–16,19]. The expression pattern and biological functions of *ANLN* in renal carcinoma remain unknown, although various studies have demonstrated that *ANLN* deregulation results in aberrant cell proliferation.

Available evidence suggests that *ANLN* is necessary for tumour cell growth and that its aberrant expression leads to the dysregulation of cell division [47]. We found that *ANLN* expression was significantly increased in ccRCC tissues compared to normal samples, which is consistent with *ANLN* expression in multiple cancers [48–50]. Moreover, upregulation of *ANLN* expression predicts an unfavorable prognosis in these patients [19]. *ANLN* expression differed among patients with renal cancer at different pathological stages, including our verification cohort and the TCGA-KIRC cohort. Additionally, *ANLN* expression differed significantly between patients with ccRCC with different pathological characteristics. *ANLN* expression is associated with ccRCC subtypes, particularly in patients with the ccB subtype. Multiple solid malignancies have revealed that *ANLN* has oncogenic effects, and *ANLN* overexpression disrupts cell division, which may be a key mechanism in cancer development [48]. In patients with colorectal cancer, increased *ANLN* expression leads to cancer invasion and enlarged tumour size [17]. The clinical samples used in the current study revealed that the tumour tissues had significantly higher levels of *ANLN* expression. *ANLN* expression varies in patients with renal cancer at different pathological stages, which prompted us to further study the effects of *ANLN* in these patients. However, survival analysis of the renal cancer cohort could not be performed owing to insufficient follow-up data. Furthermore, as the verification cohort had a short follow-up period, instances of recurrence and mortality were uncommon. Our findings from the TCGA-KIRC cohort suggest that *ANLN* expression may be a prognostic factor for these patients. Better prognosis was associated with renal carcinoma cells expressing *ANLN* in the cytoplasm [51]. The results of multivariate analysis were unremarkable; however, univariate analysis revealed that *ANLN* expression may negatively affect the prognosis of patients with ccRCC. These results can be attributed to the small sample size. These findings confirmed that *ANLN* expression can affect the prognosis of patients with ccRCC.

Despite the advances in targeted therapies, improving the overall prognosis of patients with renal cancer remains a major challenge

[52]. Immune cell infiltration is closely associated with tumour progression and treatment; however, there are few reports on the association between *ANLN* expression and the TME in patients with RCC. Our results suggest that *ANLN* expression is positively correlated with the three immune-related scores, and these scores differ significantly between patients with ccRCC with high and low *ANLN* expression. Immune cells interact with each other and the host immune system to control and influence cancer progression [53]. The immune cell landscape revealed a strong correlation between *ANLN* overexpression and number of M2 macrophages. The prognosis of patients with metastatic ccRCC is affected by the mutual aggregation of CD68⁺ tumour-associated macrophages and tumour cells [54]. Targeting macrophages is a promising strategy because of their key carcinogenic roles in tumour progression [55]. *ANLN* expression was positively correlated with the M2-type macrophage surface marker CD163 in ccRCC tissues, indicating that *ANLN* may play a role in the polarisation of M2 macrophages. Immunotherapy responses generally depend on the interaction between tumour cells and TME in human cancers [23,56,57]. Owing to the high immunogenicity of renal carcinoma, the immunosuppressive milieu in which these patients are treated can have a major impact on their clinical outcomes [5,58]. We discovered that the dysregulation of *ANLN*, particularly in PD1⁺ patients with ccRCC, is substantially affected by numerous ICIs and may influence their response to immunotherapy. All these findings indicate that *ANLN* is a potential regulator of immune cell-induced tumour escape and one of the primary mechanisms driving tumour spread.

Impaired cell cycle pathways can result in unchecked cell proliferation and, eventually, the development of malignancy [49,59]. Previous studies have shown that *ANLN* silencing causes G2/M phase arrest and suppression of cyclin-related proteins [60,61]. The PI3K-Akt pathways and cell cycle-related functions were highly enriched in these patients, which supports the findings of the aforementioned study. In particular, the abnormal activation of the PI3K/Akt/mTOR signalling pathway, a cancer driver involved in tumour growth, frequently results in severe diseases [62,63]. We further confirmed that silencing of *ANLN* expression inhibited the carcinogenesis of renal cancer cells by regulating the PI3K/AKT/mTOR pathway, indicating that *ANLN* may represent a novel target for pharmaceutical research. Nevertheless, additional research is required to support our findings, and we must consider the impact of other possible factors controlling *ANLN* expression. To further support the transcriptome findings, we also needed to increase the number of clinical samples.

5. Conclusions

In summary, our results suggest that *ANLN* is dysregulated in renal cancer tissues and promotes tumour progression via the PI3K/Akt/mTOR signalling pathway.

Funding

This study was supported by the Health Research Program of Anhui (AHWJ2022b048).

Data availability statement

Data included in article/supplementary material/referenced in article.

CRedit authorship contribution statement

Mingzhu Gao: Writing – original draft, Visualization, Software, Resources. **Zhouting Tuo:** Writing – original draft, Validation, Software, Resources. **Zhiwei Jiang:** Writing – original draft, Visualization, Validation, Software, Resources. **Zhendong Chen:** Writing – review & editing, Writing – original draft, Conceptualization. **Jinyou Wang:** Writing – review & editing, Writing – original draft, Visualization, Supervision, Software, Data curation, Conceptualization.

Declaration of competing interest

The authors declare that they have no known competing financial interests or personal relationships that could have appeared to influence the work reported in this paper.

Acknowledgements

We would like to thank Editage (www.editage.cn) for English language editing.

Appendix A. Supplementary data

Supplementary data to this article can be found online at <https://doi.org/10.1016/j.heliyon.2023.e23522>.

References

- [1] H. Zi, S.H. He, X.Y. Leng, et al., Global, regional, and national burden of kidney, bladder, and prostate cancers and their attributable risk factors, 1990–2019, *MIL MED RES* 8 (1) (2021) 60.
- [2] N. Liu, Y. Chen, L. Yang, et al., Both SUMOylation and ubiquitination of TFE3 fusion protein regulated by androgen receptor are the potential target in the therapy of Xp11.2 translocation renal cell carcinoma, *Clin. Transl. Med.* 12 (4) (2022) e797.
- [3] X. Pan, B. Huang, Q. Ma, et al., Circular RNA circ-TNPO3 inhibits clear cell renal cell carcinoma metastasis by binding to IGF2BP2 and destabilizing SERPINH1 mRNA, *Clin. Transl. Med.* 12 (7) (2022) e994.
- [4] Y. He, Y. Luo, L. Huang, et al., New frontiers against sorafenib resistance in renal cell carcinoma: from molecular mechanisms to predictive biomarkers, *Pharmacol. Res.* 170 (2021), 105732.
- [5] B. Ljungberg, L. Albiges, Y. Abu-Ghanem, et al., European Association of Urology guidelines on renal cell carcinoma: the 2022 update, *Eur. Urol.* 82 (4) (2022) 399–410.
- [6] X. Shi, D. Feng, D. Li, et al., The role of lymph node dissection for non-metastatic renal cell carcinoma: an updated systematic review and meta-analysis, *Front. Oncol.* 11 (2021), 790381.
- [7] P.C. Barata, B.I. Rini, Treatment of renal cell carcinoma: current status and future directions, *Ca - Cancer J. Clin.* 67 (6) (2017) 507–524.
- [8] J.M. Randall, F. Millard, R. Kurzrock, Molecular aberrations, targeted therapy, and renal cell carcinoma: current state-of-the-art, *CANCER METAST, Rev.* 4 (33) (2014) 1109–1124.
- [9] C.X. Li, J.S. Wang, W.N. Wang, et al., Expression dynamics of periodic transcripts during cancer cell cycle progression and their correlation with anticancer drug sensitivity, *MIL MED RES* 9 (1) (2022) 71.
- [10] J. Liu, Y. Peng, W. Wei, Cell cycle on the crossroad of tumorigenesis and cancer therapy, *Trends Cell Biol.* 32 (1) (2022) 30–44.
- [11] A.J. Piekny, M. Glotzer, Anillin is a scaffold protein that links RhoA, actin, and myosin during cytokinesis, *Curr. Biol.* 18 (1) (2008) 30–36.
- [12] A.J. Piekny, A.S. Maddox, The myriad roles of Anillin during cytokinesis, *Semin. Cell Dev. Biol.* 21 (9) (2010) 881–891.
- [13] K. Oegema, M.S. Savoian, T.J. Mitchison, et al., Functional analysis of a human homologue of the *Drosophila* actin binding protein anillin suggests a role in cytokinesis, *J. Cell Biol.* 150 (3) (2000) 539–552.
- [14] Y. Nie, Z. Zhao, M. Chen, et al., Anillin is a prognostic factor and is correlated with genovariation in pancreatic cancer based on databases analysis, *Oncol. Lett.* 21 (2) (2021) 107.
- [15] A. Maryam, Y.R. Chin, ANLN enhances triple-negative breast cancer stemness through TWIST1 and BMP2 and promotes its spheroid growth, *Front. Mol. Biosci.* 8 (2021), 700973.
- [16] J. Xu, H. Zheng, S. Yuan, et al., Overexpression of ANLN in lung adenocarcinoma is associated with metastasis, *THORAC CANCER* 10 (8) (2019) 1702–1709.
- [17] G. Wang, W. Shen, L. Cui, et al., Overexpression of Anillin (ANLN) is correlated with colorectal cancer progression and poor prognosis, *CANCER BIOMARK* 16 (3) (2016) 459–465.
- [18] X. Dai, Y. Mei, X. Chen, et al., ANLN and KDR are jointly prognostic of breast cancer survival and can be modulated for triple negative breast cancer control, *Front. Genet.* 10 (2019) 790.
- [19] K. Liu, L. Cui, C. Li, et al., Pan-cancer analysis of the prognostic and immunological role of ANLN: an onco-immunological biomarker, *Front. Genet.* 13 (2022), 922472.
- [20] X. Li, X. Geng, Z. Chen, et al., Recent advances in glioma microenvironment-response nanoplatforms for phototherapy and sonotherapy, *Pharmacol. Res.* 179 (2022), 106218.
- [21] H. Ye, X. Hu, Y. Wen, et al., Exosomes in the tumor microenvironment of sarcoma: from biological functions to clinical applications, *J NANOBIO TECHNOLOGY* 20 (1) (2022) 403.
- [22] S. Paul, S. Sinha, C.N. Kundu, Targeting cancer stem cells in the tumor microenvironment: an emerging role of PARP inhibitors, *Pharmacol. Res.* 184 (2022), 106425.
- [23] L. Lisi, P.M. Lecal, M. Martire, et al., Clinical experience with CTLA-4 blockade for cancer immunotherapy: from the monospecific monoclonal antibody ipilimumab to probodies and bispecific molecules targeting the tumor microenvironment, *Pharmacol. Res.* 175 (2022), 105997.
- [24] S. Xing, K. Hu, Y. Wang, Tumor immune microenvironment and immunotherapy in non-small cell lung cancer: update and new challenges, *AGING DIS* 13 (6) (2022) 1615–1632.
- [25] D. Ti, X. Yan, J. Wei, et al., Inducing immunogenic cell death in immuno-oncological therapies, *Chin. J. Cancer Res.* 34 (1) (2022) 1–10.
- [26] Y. Qian, T. Yang, H. Liang, et al., Myeloid checkpoints for cancer immunotherapy, *Chin. J. Cancer Res.* 34 (5) (2022) 460–482.
- [27] Z. Tuo, Y. Zhang, X. Wang, et al., RUNX1 is a promising prognostic biomarker and related to immune infiltrates of cancer-associated fibroblasts in human cancers, *BMC Cancer* 22 (1) (2022) 523.
- [28] M.J. Goldman, B. Craft, M. Hastie, et al., Visualizing and interpreting cancer genomics data via the Xena platform, *Nat. Biotechnol.* 38 (6) (2020) 675–678.
- [29] S.J. Park, B.H. Yoon, S.K. Kim, et al., GENT2: an updated gene expression database for normal and tumor tissues, *BMC MED GENOMICS Suppl* 5 (12) (2019) 101.
- [30] J. Barretina, G. Caponigro, N. Stransky, et al., The Cancer Cell Line Encyclopedia enables predictive modelling of anticancer drug sensitivity, *Nature* 483 (7391) (2012) 603.
- [31] D.S. Chandrashekar, B. Bashel, S.A.H. Balasubramanya, et al., UALCAN: a portal for facilitating tumor subgroup gene expression and survival analyses, *Neoplasia* 19 (8) (2017) 649–658.
- [32] S.H. Liu, P.C. Shen, C.Y. Chen, et al., DriverDBv3: a multi-omics database for cancer driver gene research, *Nucleic Acids Res.* 48 (D1) (2020) D863.
- [33] V. Thorsson, D.L. Gibbs, S.D. Brown, et al., The immune landscape of cancer, *Immunity* 4 (48) (2018) 812–830.
- [34] R. Beroukhi, C.H. Mermel, D. Porter, et al., The landscape of somatic copy-number alteration across human cancers, *Nature* 463 (7283) (2010) 899–905.
- [35] A. Mayakonda, D.C. Lin, Y. Assenov, et al., Maftools: efficient and comprehensive analysis of somatic variants in cancer, *Genome Res.* 28 (11) (2018) 1747–1756.
- [36] G. Yu, L.G. Wang, Y. Han, et al., clusterProfiler: an R package for comparing biological themes among gene clusters, *OMICS* 16 (5) (2012) 284–287.
- [37] Y. Lin, Y. Zhang, Z. Tuo, et al., ORC6, a novel prognostic biomarker, correlates with T regulatory cell infiltration in prostate adenocarcinoma: a pan-cancer analysis, *BMC Cancer* 23 (1) (2023) 285.
- [38] C. Liu, S. Dai, H. Geng, et al., Development and validation of a kidney renal clear cell carcinoma prognostic model relying on pyroptosis-related lncRNAs-A multidimensional comprehensive bioinformatics exploration, *Eur. J. Med. Res.* 28 (1) (2023) 341.
- [39] J. Wu, L. Li, H. Zhang, et al., A risk model developed based on tumor microenvironment predicts overall survival and associates with tumor immunity of patients with lung adenocarcinoma, *Oncogene* 40 (26) (2021) 4413–4424.
- [40] A.M. Newman, C.L. Liu, M.R. Green, et al., Robust enumeration of cell subsets from tissue expression profiles, *Nat. Methods* 12 (5) (2015) 453–457.
- [41] P. Charoentong, F. Finotello, M. Angelova, et al., Pan-cancer immunogenomic analyses reveal genotype-immunophenotype relationships and predictors of response to checkpoint blockade, *Cell Rep.* 18 (1) (2017) 248–262.
- [42] P. Geeleher, N. Cox, R.S. Huang, pRRophetic: an R package for prediction of clinical chemotherapeutic response from tumor gene expression levels, *PLoS One* 9 (9) (2014), e107468.
- [43] X. Chen, J. Zhang, X. Lei, et al., CD1C is associated with breast cancer prognosis and immune infiltrates, *BMC Cancer* 23 (1) (2023) 129.
- [44] P.H. Li, X.Y. Kong, Y.Z. He, et al., Recent developments in application of single-cell RNA sequencing in the tumour immune microenvironment and cancer therapy, *MIL MED RES* 9 (1) (2022) 52.
- [45] A.M. Raghobar, M.J. Roberts, S. Wood, et al., Cellular milieu in clear cell renal cell carcinoma, *Front. Oncol.* 12 (2022), 943583.
- [46] D Heng V Navani, Treatment selection in first-line metastatic renal cell carcinoma-the contemporary treatment paradigm in the age of combination therapy: a review, *JAMA Oncol.* 8 (2) (2022) 292.

- [47] J.X. Xiao, W. Xu, X. Fei, et al., Anillin facilitates cell proliferation and induces tumor growth of hepatocellular carcinoma via miR-138/SOX4 axis regulation, *TRANSL ONCOL* 13 (10) (2020), 100815.
- [48] Naydenov Ng, J.E. Koblinski, A.I. Ivanov, Anillin is an emerging regulator of tumorigenesis, acting as a cortical cytoskeletal scaffold and a nuclear modulator of cancer cell differentiation, *Cell. Mol. Life Sci.* 78 (2) (2021) 621.
- [49] B. Wang, X.L. Zhang, C.X. Li, et al., ANLN promotes carcinogenesis in oral cancer by regulating the PI3K/mTOR signaling pathway, *Head Face Med.* 17 (1) (2021) 18.
- [50] D. Wang, Naydenov Ng, M.G. Dozmorov, et al., Anillin regulates breast cancer cell migration, growth, and metastasis by non-canonical mechanisms involving control of cell stemness and differentiation, *Breast Cancer Res.* 22 (1) (2020) 3.
- [51] H. Ronkainen, P. Hirvikoski, S. Kauppila, et al., Anillin expression is a marker of favourable prognosis in patients with renal cell carcinoma, *Oncol. Rep.* 25 (1) (2011) 129–133.
- [52] M. Rosellini, A. Marchetti, V. Mollica, et al., Prognostic and predictive biomarkers for immunotherapy in advanced renal cell carcinoma, *Nat. Rev. Urol.* 20 (3) (2023) 133–157.
- [53] D'Andrea Ma, G.K. Reddy, Immune system activation in patients with metastatic renal cell carcinoma induced by the systemic abscopal effects of radiation therapy, *Oncol. Res. Treat.* 46 (1–2) (2023) 33–44.
- [54] N.H. Chakiryan, G.J. Kimmel, Y. Kim, et al., Spatial clustering of CD68+ tumor associated macrophages with tumor cells is associated with worse overall survival in metastatic clear cell renal cell carcinoma, *PLoS One* 4 (16) (2021), e245415.
- [55] B. Li, S. Sun, J.J. Li, et al., Adipose tissue macrophages: implications for obesity-associated cancer, *MIL MED RES* 10 (1) (2023) 1.
- [56] Y. Wang, F. Gao, X. Li, et al., Tumor microenvironment-responsive fenton nanocatalysts for intensified anticancer treatment, *J NANOBIO TECHNOLOGY* 20 (1) (2022) 69.
- [57] L. Liu, Y. Qu, L. Cheng, et al., Engineering chimeric antigen receptor T cells for solid tumour therapy, *Clin. Transl. Med.* 12 (12) (2022) e1141.
- [58] T. Wu, Y. Dai, Tumor microenvironment and therapeutic response, *Cancer Lett.* 387 (2017) 61–68.
- [59] L. Su, Z. Sun, F. Qi, et al., GRP75-driven, cell-cycle-dependent macropinocytosis of Tat/pDNA-Ca(2+) nanoparticles underlies distinct gene therapy effect in ovarian cancer, *J. Nanobiotechnol.* 1 (20) (2022) 340.
- [60] S. Zeng, X. Yu, C. Ma, et al., Transcriptome sequencing identifies ANLN as a promising prognostic biomarker in bladder urothelial carcinoma, *SCI REP-UK* 1 (7) (2017) 3151.
- [61] K. Magnusson, G. Gremel, L. Rydén, et al., ANLN is a prognostic biomarker independent of Ki-67 and essential for cell cycle progression in primary breast cancer, *BMC Cancer* 16 (1) (2016) 904.
- [62] G. Liu, X. Li, F. Yang, et al., C-phycocyanin ameliorates the senescence of mesenchymal stem cells through ZDHHC5-mediated autophagy via PI3K/AKT/mTOR pathway, *AGING DIS* 14 (4) (2023) 1425–1440.
- [63] J. Yang, J. Nie, X. Ma, et al., Targeting PI3K in cancer: mechanisms and advances in clinical trials, *Mol. Cancer* 18 (1) (2019) 26.